Noise Properties in SESAM-Based Mode-Locked Laser With Intracavity Pump Reflection Coating

Di Yang, Kan Wu, Ming Tang, *Senior Member, IEEE*, Perry Ping Shum, *Senior Member, IEEE*, Songnian Fu, and Deming Liu

***Abstract*— We investigate the intensity noise and microwave phase noise properties in an SESAM-based mode-locked fiber laser operating at 1.55 μm with intracavity pump reflection coating. Two lasers with similar design are made for comparison with one having a pump reflection coating whereas the other one has not. The noise conversion from pump relative intensity noise (RIN) to the RIN and phase noise of two lasers is evaluated experimentally. It is found that although the laser with pump reflection coating has much lower self-starting pump power and higher slope pumping efficiency, the pump-RIN-to-laser-RIN conversion scales as the square of the slope efficiency at low-frequency region and thus is increased by ∼7 dB in the laser with coating. The pump-RIN-to-laser-phase-noise conversion is also increased due to the existence of the slow saturable absorber effect.**

***Index Terms*— Laser noises, mode-locked lasers, ultrafast lasers.**

I. Introduction

THE demand for mode-locked fiber lasers (MLLs) with low noise, especially low intensity noise and microwave phase noise, is increasing for high-precision scientific and engineering applications such as frequency metrology [1] and coherent communication [2]. Various noise mechanisms have been investigated theoretically [3]–[5] and experimentally [6]–[12]. Meanwhile, since the invention of semiconductor saturable absorber mirror (SESAM) [13], [14], it has been widely used for passively mode-locked lasers due to the mature fabrication technology and commercial availability. Study on the compact linear-cavity lasers mode locked by SESAM has been performed and the laser noise characteristics have also been investigated [15]. Linear cavity can effectively shorten the cavity length and increase the repetition frequency of the mode-locked lasers [16]–[19]. For the SESAM-based mode-locked lasers with linear cavity and high repetition frequency (e.g., higher than 500 MHz) at 1.55 μm, the residual pump power is usually high due to the insufficient absorption in the Erbium-doped fiber (EDF). This residual pump power, if not reflected by the pump reflection coating, will be absorbed by the SESAM at the end of the laser cavity and disturb the laser operation or even damage the SESAM due to the heat accumulation on the SESAM. Therefore placing a pump reflection coating before the SESAM can effectively protect the SESAM and increase the pumping efficiency of the laser. A 1-GHz mode-locked fiber laser with pump reflection coating has been reported and very high pumping efficiency has been observed [16]. However, it is still unclear how this intra-cavity pump reflection coating affects the intensity noise and phase noise properties in such kinds of lasers and no work has been reported on this topic.

In this letter, the impacts of intra-cavity pump reflection coating are investigated by comparing the noise performance in two mode-locked fiber lasers with similar cavity design and one laser has pump reflection coating before the SESAM whereas the other has not. Pump modulation technology [15] is applied to evaluate the noise conversion process from the pump RIN to the laser RIN and microwave phase noise (corresponds to timing jitter of the pulse train). It is observed that the threshold of the laser with pump reflection coating is significantly reduced and the slope pumping efficiency is also increased due to the re-use of residual pump light enabled by the pump reflection. However, the laser RIN becomes more sensitive to the noise from the pump diode. The noise conversion ratios from the pump RIN to the laser RIN is found to be ∼7 dB higher at 1 kHz offset frequency due to the existence of pump reflection coating. Phase noise conversion ratio is also increased due to the slow saturable absorber effect in the laser. Theoretical analysis is also performed to explain this phenomenon.

II. Experimental Setup and Analysis

The design of the mode-locked lasers is shown in the dashed line frame in Fig. 1. The laser cavity consists of a piece of highly-doped Erbium doped fiber (LIEKKI Er80 8/125) with anomalous dispersion and a standard single mode fiber (SMF).

Manuscript received October 21, 2014; revised January 11, 2015; accepted March 17, 2015. Date of publication March 19, 2015; date of current version May 11, 2015. This work was supported in part by the 863 High Technology Plan of China under Grant 2013AA013402, in part by the Fundamental Research Funds for the Central Universities under Grant HUST: 2013TS052, in part by the National Basic Research Program (973 Program) of China under Grant 2010CB328305, and in part by the National Natural Science Foundation of China under Grant 61107087 and Grant 61331010.

D. Yang, M. Tang, S. Fu, and D. Liu are with the Wuhan National Laboratory for Optoelectronics, Huazhong University of Science and Technology, Wuhan 430074, China, and also with the Next Generation Internet Access National Engineering Laboratory, School of Optical and Electronic Information, Huazhong University of Science and Technology, Wuhan 430074, China (e-mail: yangdil3h4@163.com; tangming@mail.hust.edu.cn; songnian@mail.hust.edu.cn; dmliu@mail.hust.edu.cn).

K. Wu is with the State Key Laboratory on Advanced Optical Communication Systems and Networks, Shanghai Jiao Tong University, Shanghai 200240 China (e-mail: hokvens@hotmail.com).

P. P. Shum is with the School of Electrical and Electronic Engineering, Nanyang Technological University, Singapore 639798 (e-mail: shum@ieee.org).

Color versions of one or more of the figures in this letter are available online at http://ieeexplore.ieee.org.

Digital Object Identifier 10.1109/LPT.2015.2414882

1041-1135 © 2015 IEEE. Personal use is permitted, but republication/redistribution requires IEEE permission.
See http://www.ieee.org/publications_standards/publications/rights/index.html for more information.

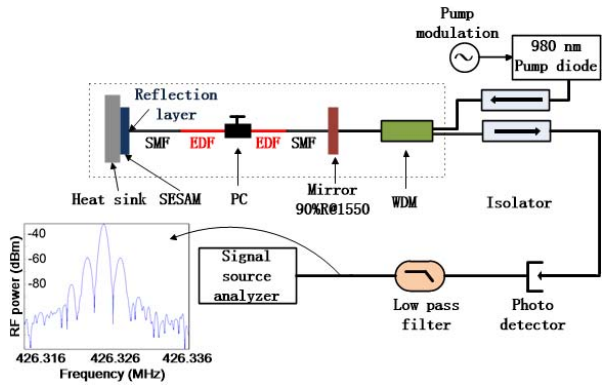

Fig. 1. Schematic diagram of the mode-locked laser design and the experimental setup for the noise characterization. The inset is an example of the RF spectrum after photodetection when a 2 kHz pump modulation is applied to the Laser A.

TABLE I
SUMMARY OF LASER A AND B

	Laser A without pump reflection coating	Laser B with pump reflection coating
Cavity	10 cm EDF + 13.5 cm SMF	10 cm EDF + 13.3 cm SMF
Mode locking threshold (mW)	193	92
Rep. frequency (MHz)	426.3	428.9
Center wavelength (nm)	1566.6	1565.2
Slope efficiency (measured at laser output)	1.71%	3.90%

The dispersion value of EDF is very close with SMF so that the laser operates at soliton mode locking regime. The length of cavity is ~23.5 cm, thus, intra-cavity dispersion is evaluated as ~ -0.00519 ps^2. The SESAM (SAM-1550-8, BATOP) is applied at the left end of the laser cavity as the mode locker and is butt coupled to the fiber end. The modulation depth of SESAM is ~6%, the chip area is 1.3mm × 1.3mm. The SESAM is protected by a dielectric front layer. Therefore, the pump reflection coating will not change the SESAM parameters as discussed in [20]. For the laser without pump reflection coating (denoted as Laser A), the SESAM was butt directly coupled to the fiber end. A Peltier cooler together with a copper heat sink is used on the back side of the SESAM to dissipate the heat generated by the residual pump power. For the laser with pump reflection coating on the fiber end before the SESAM (denoted as Laser B), only a copper heat sink can make the laser normal operate. However, in this case, we want two lasers working under the same environment. Thus, a Peltier cooler is still added for laser B. Note that the saturation fluence of the SESAM at 1550 nm is ~30 μJ/cm^2 whereas the typical fluence induced by the residue pump is ~20nJ/cm^2 (assuming 10 mW residue power). Fluence induced by the residue pump power for laser B is some orders of magnitude lower than the fluence of the 1550 nm pulses and therefore negligible. The pump reflection coating has ~95% reflection at 980 nm. On the right end of the laser cavity, a dielectric coating with 90% reflection at 1.55 μm and high transmission at 980 nm is made on the fiber end as the output coupler. 980 nm pump light is coupled into the cavity through a 980/1550 wavelength division multiplexer (WDM). The laser output is fed into the photodetector through an isolator and then filtered by a low pass filter for the noise measurement in the signal source analyzer (SSA, R&S FSUP26).

The specifications of the two lasers are summarized in Table I. It can be seen that two lasers have quite similar performance except for the very different threshold pump powers for the self-starting mode locking operation and the slope efficiency.

Pump modulation technique is adopted to quantitatively characterize the sensitivity of the laser RIN and phase noise on the pump power fluctuation [15]. As shown in Fig. 1, a weak modulation current at a given frequency f_M is added to the bias current of the pump laser diode and thus a controlled pump RIN is generated. The amplitude of the modulation current is 0.1-0.5% of the bias current. By comparing the power of the noise spur at f_M in the power spectral densities (PSDs) of pump RIN, laser RIN and laser phase noise, the noise conversion ratio from the pump to the laser can be obtained. This definition can be described as follows:

$$r_{\mathrm{RIN}}(f_M) = \frac{S_{\mathrm{RIN}}(f_M)}{S_{\mathrm{Pump-RIN}}(f_M)} \tag{1}$$

$$r_{\mathrm{PN}}(f_M) = \frac{S_{\mathrm{PN}}(f_M)}{S_{\mathrm{Pump-RIN}}(f_M)} \tag{2}$$

where $r_{\mathrm{RIN}}(f_M)$ and $r_{\mathrm{PN}}(f_M)$ are the noise conversion ratios from the pump RIN to the laser RIN and laser phase noise, respectively. $S_{\mathrm{Pump-RIN}}(f_M)$, $S_{\mathrm{RIN}}(f_M)$ and $S_{\mathrm{PN}}(f_M)$ (with the units of dBc getting from SSA) are the power of the noise spurs at f_M in the PSDs of pump RIN, laser RIN and laser phase noise, respectively. The units in Eq.(1) and (2) are linear units. The optical power is properly attenuated before it is fed into the photodetector to avoid excess RIN-to-phase-noise conversion in the photodetector [8].

The inset in Fig. 1 shows the radio frequency (RF) spectrum at the fundamental repetition frequency of Laser A when a 2 kHz pump modulation is applied. Two sidebands with 2 kHz spacing to the center frequency can be clearly observed. Similarly, we can define a conversion ratio $r_{RF}(f_M)$ from the pump RIN to the relative RF sideband power as follows:

$$r_{RF}(f_M) = \frac{P(f_R \pm f_M)/P(f_R)}{S_{\mathrm{Pump-RIN}}(f_M)} \tag{3}$$

where $P(f_R)$ is the RF power of the center frequency (i.e., the fundamental repetition frequency f_R) and $P(f_R \pm f_M)$ is the RF power of the sidebands generated by the pump modulation. Since the power of these RF sidebands equal to the sum of the power of RIN and phase noise spurs in the laser noise spectra, the following relation is satisfied at all modulation

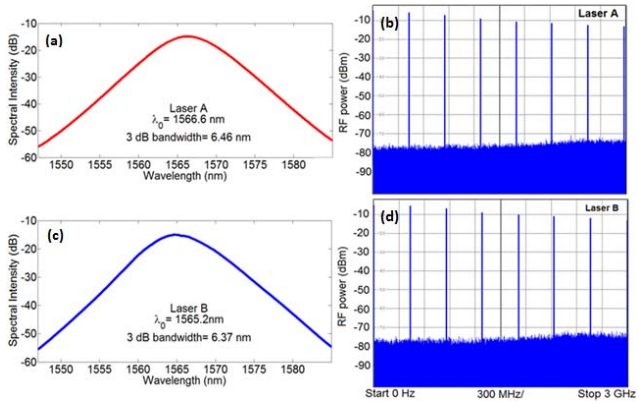

Fig. 2. (a) (c) Optical spectrum of laser A and B. (b) (d) Corresponding output RF spectrum of the photodetector, the resolution bandwidth is 10 kHz.

frequency f_M:

$$r_{RF} = r_{\mathrm{RIN}} + r_{\mathrm{PN}} \tag{4}$$

This relation can be used to verify the correctness of the laser RIN and phase noise measurement.

For a controlled study, the parameters of two lasers have to be kept as similar as possible. Thus, one same pump diode is used. Since the threshold of two lasers is significantly different, the pump power is tuned to make the output parameters as close as possible. The optical spectrums are shown in Fig. 2(a) while Fig. 2(b) are the corresponding RF spectrums. The pump power for laser A is ∼310mW and for laser B is ∼140mW.

The measured noise conversion ratio for Laser A without pump reflection coating is shown in Fig. 3(a). The RIN conversion ratio r_{RIN} is flat in the low offset frequency region and decays quickly in the high offset frequency range. While the phase noise conversion ratio r_{PN} keeps decaying quickly in the whole frequency region. These properties are consistent with the results reported in our previous work [15]. It can be also observed that the conversion ratio of the relative RF sideband power r_{RF} is indeed equal to the sum of the RIN and phase noise conversion ratios, which confirms the validity of the noise measurement results.

With the noise conversion ratios and pump RIN spectrum known, one can predict the laser RIN and phase noise spectra according to Eqs.(1) and (2), as shown in Fig. 3(b). It can be observed that the predicted noise PSDs fit well with the measured noise PSDs which confirms the correctness of the results. The deviation in noise PSD at the offset frequencies greater than 20 kHz is due to the noise floor limitation in the measurement.

It should be noted that due to the existence of excess RIN-to-phase-noise conversion caused by the slow saturable absorber effect shown in Ref. [15], the phase noise spectrum is dominated by this effect and thus different from those measured in the lasers mode locked by nonlinear effects such as soft Kerr mode locking in the Ti: Sapphire laser [21] and nonlinear polarization rotation (NPR) in the fiber laser [15]. The calculated phase noise PSD induced by the slow saturable absorber effect ΔS_{PN} is also plotted in Fig. 3(b) and is very close to the measured phase noise PSD. The expression of

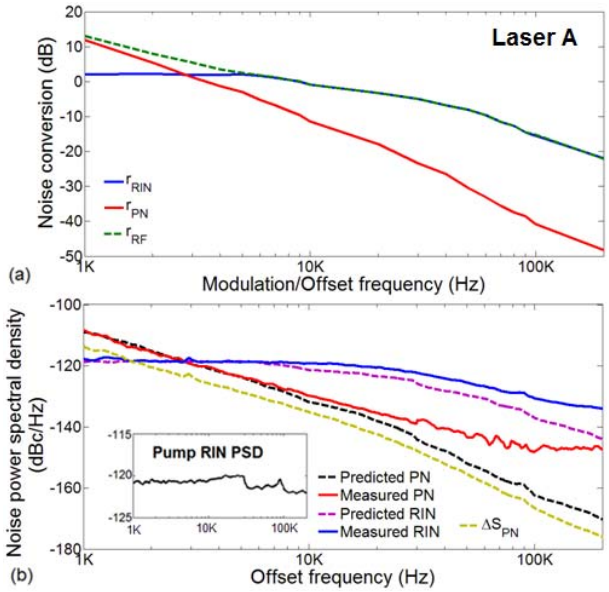

Fig. 3. (a) Noise conversion ratios measured for Laser A without pump reflection coating and (b) measured and predicted PSDs of the laser RIN and phase noise. ΔSPN is the phase noise induced by the slow saturable absorber effect. Inset is the PSD of pump RIN.

ΔS_{PN} is given by

$$\begin{aligned}\Delta S_{\mathrm{PN}}(f) &= 20\lg(f_{rep}^2 \frac{\partial \Delta t}{\partial s} s) - 20\lg f + S_{\mathrm{RIN}}(f) \\ &= 64.1dB - 20\lg f + S_{\mathrm{RIN}}(f)\end{aligned} \tag{5}$$

where f_{rep} and f is the repetition frequency and offset frequency respectively, S_{RIN} is the laser RIN PSD. The parameters used are $s = \mathrm{Ep/Es} = 2.44$ and $\partial\Delta t/\partial s = 3.6fs$ where s is the saturation parameter equal to the ratio of intra-cavity pulse energy Ep = 117 pJ and saturation energy Es = 48pJ of the SESAM and $\partial\Delta t/\partial s$ is the slope of slow saturable absorber effect induced temporal shift Δt with respect to s [5]. The difference is probably due to the error in the estimation of these parameters. Note that the typical value for the saturation parameter s to eliminate the noise coupling is ∼2.9, the slope $\partial\Delta t/\partial s$ becomes zero at this point. But one should also note that for the lasers whose saturable absorbers are deeply saturated, i.e., s≫2.9, deliberately pushing s to 2.9 will sacrifice the output power as well as output bandwidth.

For Laser B, the measured noise conversion ratios are shown in Fig. 4(a). It can be seen that the noise conversion from the pump RIN to the laser RIN (r_{RIN}) is ∼7 dB higher than that of Laser A without pump reflection coating at 1 kHz offset frequency. The expression of ΔS_{PN} for laser B is the same with laser A since the same structure design. The RIN conversion ratio can be modeled as follows (see Eq.(A.12) in Ref [22])

$$r_{\mathrm{RIN}} = \frac{\eta^2}{1 + \frac{\gamma_{sp}^2 - 2\omega_{sp}^2}{\omega_{sp}^4}\omega_m^2 + \frac{\omega_m^4}{\omega_{sp}^4}} \tag{6}$$

where η is a parameter representing the pumping efficiency, γ_{sp} is a parameter related to the spontaneous emission, ω_{sp} is the roll-off (angular) frequency of the RIN conversion which is related to the spontaneous emission and photon life time in the laser cavity, ω_m is the modulation (angular) frequency.

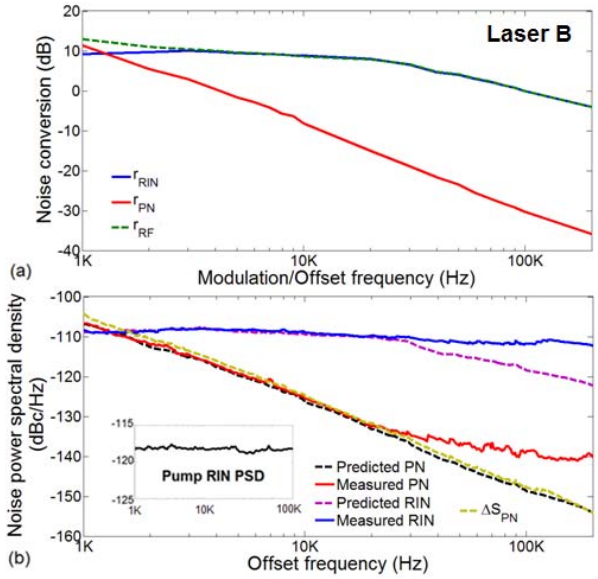

Fig. 4. (a) Noise conversion ratios measured for laser B and (b) measured and predicted PSDs of the laser RIN and phase noise. ΔSPN is the phase noise induced by the slow saturable absorber effect. Inset is the PSD of pump RIN.

7 dB increase (or 5.0 times higher in the linear scale) of RIN conversion ratio means η of Laser B is ∼2.24 times higher than that of Laser A, which is consistent with the observation that the slope efficiency of Laser B is ∼2.28 times higher than that of Laser A. This means the RIN conversion ratio scales as the square of the slope efficiency at low-offset frequency region.

The conversion ratio of the relative RF sideband power is also plotted and is indeed equal to the sum of r_{RIN} and r_{PN}, which again confirms the validity of the noise measurement. Similarly, with the measured noise conversion ratios and the pump RIN PSD, one can predict the laser RIN and phase noise using Eqs. (1) and (2), shown in Fig. 4(b). The predicted and measured noise PSDs fit well with each other. The deviation after 20 kHz is due to the noise floor of the measurement system. Inset is the PSD of pump RIN, it increases ∼3dB at 1 kHz comparing to that of laser A. This is caused by the pump diode working at a relatively low power for laser B. Under this condition, the RIN PSD improves both in low and high frequency region. However, it does not affect the final result since noise conversion is a difference value.

Thus, for two lasers with identical design except for the pump reflection coating, the pump reflection coating can benefit the slope efficiency on the cost of worse pump RIN to laser RIN conversion

III. Conclusion

In conclusion, we experimentally investigate the intensity noise and phase noise properties in a SESAM-based mode-locked fiber laser at 1.55 μm with intra-cavity pump reflection coating. Two mode-locked fiber lasers with similar linear cavity design are compared when one has an intra-cavity pump reflection coating and the other hasn't. It is found that although intra-cavity pump reflection coating can effectively reduce the mode locking threshold and increase the slope pumping efficiency, it also results in worse noise conversion from the pump RIN to the laser RIN, which scales as the square of the slope efficiency at low-offset frequency region. The noise conversion from the pump RIN to the laser phase noise also becomes higher due to the existence of slow saturable absorber effect.

References

[1] R. Holzwarth, M. Zimmermann, T. Udem, and T. W. Hansch, "Optical clockworks and the measurement of laser frequencies with a mode-locked frequency comb," *IEEE J. Quantum Electron.*, vol. 37, no. 12, pp. 1493–1501, Dec. 2001.

[2] K. Kikuchi and S. Tsukamoto, "Evaluation of sensitivity of the digital coherent receiver," *J. Lightw. Technol.*, vol. 26, no. 13, pp. 1817–1822, Jul. 1, 2008.

[3] H. A. Haus and A. Mecozzi, "Noise of mode-locked lasers," *IEEE J. Quantum Electron.*, vol. 29, no. 3, pp. 983–996, Mar. 1993.

[4] R. Paschotta, "Noise of mode-locked lasers (Part I): Numerical model," *Appl. Phys. B*, vol. 79, no. 2, pp. 153–162, Jul. 2004.

[5] R. Paschotta, "Noise of mode-locked lasers (Part II): Timing jitter and other fluctuations," *Appl. Phys. B*, vol. 79, no. 2, pp. 163–173, Jul. 2004.

[6] R. P. Scott, T. D. Mulder, K. A. Baker, and B. H. Kolner, "Amplitude and phase noise sensitivity of modelocked Ti: Sapphire lasers in terms of a complex noise transfer function," *Opt. Exp.*, vol. 15, no. 14, pp. 9090–9095, 2007.

[7] K. Wu, C. Ouyang, J. H. Wong, S. Aditya, and P. Shum, "Frequency response of the noise conversion from relative intensity noise to phase noise in the photodetection of an optical pulse train," *IEEE Photon. Technol. Lett.*, vol. 23, no. 8, pp. 468–470, Apr. 15, 2011.

[8] K. Wu *et al.*, "Characterization of the excess noise conversion from optical relative intensity noise in the photodetection of mode-locked lasers for microwave signal synthesis," *J. Lightw. Technol.*, vol. 29, no. 24, pp. 3622–3631, Dec. 15, 2011.

[9] K. Wu *et al.*, "Nonlinear coupling of relative intensity noise from pump to a fiber ring laser mode-locked with carbon nanotubes," *Opt. Exp.*, vol. 18, no. 16, pp. 16663–16670, 2010.

[10] K. Wu *et al.*, "Timing-jitter reduction of passively mode-locked fiber laser with a carbon nanotube saturable absorber by optimization of cavity loss," *Opt. Lett.*, vol. 35, no. 7, pp. 1085–1087, 2010.

[11] C. Kim, S. Bae, K. Kieu, and J. Kim, "Sub-femtosecond timing jitter, all-fiber, CNT-mode-locked Er-laser at telecom wavelength," *Opt. Exp.*, vol. 21, no. 22, pp. 26533–26541, Nov. 2013.

[12] C. Kim, K. Jung, K. Kieu, and J. Kim, "Low timing jitter and intensity noise from a soliton Er-fiber laser mode-locked by a fiber taper carbon nanotube saturable absorber," *Opt. Exp.*, vol. 20, no. 28, pp. 29524–29530, Dec. 2012.

[13] U. Keller, D. A. B. Miller, G. D. Boyd, T. H. Chiu, J. F. Ferguson, and M. T. Asom, "Solid-state low-loss intracavity saturable absorber for Nd:YLF lasers: An antiresonant semiconductor Fabry–Perot saturable absorber," *Opt. Lett.*, vol. 17, no. 7, pp. 505–507, Apr. 1992.

[14] U. Keller *et al.*, "Semiconductor saturable absorber mirrors (SESAM's) for femtosecond to nanosecond pulse generation in solid-state lasers," *IEEE J. Sel. Top. Quantum Electron.*, vol. 2, no. 3, pp. 435–453, Sep. 1996.

[15] K. Wu *et al.*, "Noise conversion from pump to the passively mode-locked fiber lasers at 1.5 μm," *Opt. Lett.*, vol. 37, no. 11, pp. 1901–1903, 2012.

[16] H. Byun *et al.*, "Compact, stable 1 GHz femtosecond Er-doped fiber lasers," *Appl. Opt.*, vol. 49, no. 29, pp. 5577–5582, 2010.

[17] A. Martinez and Z. Sun, "Nanotube and graphene saturable absorbers for fibre lasers," *Nature Photon.*, vol. 7, pp. 842–845, Oct. 2013.

[18] A. Martinez and S. Yamashita, "Multi-gigahertz repetition rate passively modelocked fiber lasers using carbon nanotubes," *Opt. Exp.*, vol. 19, no. 7, pp. 6155–6163, Mar. 2011.

[19] B. C. Collings *et al.*, "Short cavity erbium/ytterbium fiber lasers mode-locked with a saturable Bragg reflector," *IEEE J. Sel. Topics Quantum Electron.*, vol. 3, no. 4, pp. 1065–1075, Aug. 1997.

[20] G. J. Spühler *et al.*, "Semiconductor saturable absorber mirror structures with low saturation fluence," *Appl. Phys. B*, vol. 81, no. 1, pp. 27–32, Jul. 2005.

[21] T. D. Mulder, R. P. Scott, and B. H. Kolner, "Amplitude and envelope phase noise of a modelocked laser predicted from its noise transfer function and the pump noise power spectrum," *Opt. Exp.*, vol. 16, no. 18, pp. 14186–14191, Sep. 2008.

[22] K. Wu, *Ultra-Low Jitter Mode-Locked Fiber Laser*. Singapore: Nanyang Technol. Univ., 2012. [Online]. Available: http://hdl.handle.net/10356/50805